

Supporting Information

μ -Oxo Hetero Dimer of Silicon Phthalocyanine and Naphthalocyanine

Kazuaki Oniwa,^a Soji Shimizu,^{a*} Yuta Shiina,^a Takamitsu Fukuda,^b and Nagao Kobayashi^{a*}

^a*Department of Chemistry, Graduate School of Science, Tohoku University, Sendai 980-8578, Japan*

^b*Department of Chemistry, Graduate School of Science, Osaka University, Toyonaka 560-0043, Japan*

Contents:

- i. Experimental
- ii. Space filling model of the crystal structure of **6**
- iii. Absorption and MCD spectra of **1** and **2**
- iv. Absorption spectra of **6** at variable concentrations
- v. ¹H NMR spectra of **6** and variable temperature measurements
- vi. Absorption spectra of **6** at variable temperatures
- vii. DFT and TDDFT calculations on **6**
- viii. References
- ix. Acknowledgement

i. Experimental

General procedure: Electronic absorption spectra were recorded on a JASCO V-570 spectrophotometer. Magnetic circular dichroism (MCD) spectra were recorded in the UV/vis/NIR region on a JASCO J-725 spectrodichrometer equipped with a JASCO electromagnet, which produces magnetic fields of up to 1.03 T (1 T = 1 tesla) and in the vis/NIR region on a JASCO J-730 spectrodichrometer equipped with a JASCO electromagnet that produce magnetic fields of up to 1.5 T with both parallel and antiparallel fields. The magnitudes were expressed in terms of molar ellipticity per tesla ($[\theta]_M / \text{deg dm}^3 \text{ mol}^{-1} \text{ T}^{-1}$). ¹H NMR and ¹H-¹H COSY spectra were recorded on a JEOL ECA-600 spectrometer (operating at 594.17 MHz), and Bruker AVANCE 600 (operating at 600.13 MHz) and AVANCE 400 (operating at 400.33 MHz) spectrometers using the residual solvent as the internal reference for ¹H ($\delta = 7.26$ ppm for CDCl₃ and $\delta = 2.09$ ppm for toluene-*d*₈). High resolution mass spectra were recorded on a Bruker Daltonics Apex-III spectrometer. Preparative separations were performed by alumina gel column chromatography (Wako), Bio-Beads (S-X1), and recycling preparative GPC-HPLC (JAI LC-9201 with preparative JAIGEL-2H, 2.5H, and 3H columns). All reagents and solvents were of commercial reagent grade and were used without further purification except where noted.

Crystallographic data collection and structure refinement: Data collection for **6** was carried out at -173(2) °C on a Bruker APEXII CCD diffractometer with MoK α radiation ($\lambda = 0.71073$ Å). The structure was solved by direct methods (Sir 2004)¹ and refined using a full-matrix least square technique (SHELXL-97).² Solvent molecules in the lattice of **6** were severely disordered and could not be resolved. The program SQUEEZE in PLATON³ was used to remove the solvent electron density. The peripheral butoxy

substituents were severely disordered despite the low measurement temperature. Therefore, the structure was refined under thermally and positionally restrained conditions, using ANTIBUMP, DFIX, SIMU, ISOR, and DELU commands. There are 1119 restraints in the final refinement, of which 15 for ANTIBUMP, 114 for DFIX, 114 for DELU, 402 for SIMU, and 474 for ISOR commands. After the above-mentioned refinement, one electron density with 1.01 was still observed, and two A level alerts arose in the cif check due to the disorder of the butoxy substituents.

Computational methods: The Gaussian 09 software package⁴ was utilized for DFT and TDDFT calculations using the B3LYP functional with 6-31G(d) basis set. Structural optimization was performed on model compounds of **6** in which the peripheral butoxy substituents and axial ligands were replaced by hydrogen and chloride atoms, respectively, for simplicity.

Dihydroxy(octakisbutoxyphthalocyanato)silicon (1): To a suspension of 5,6-dibutoxy-1,3-diiminoisoindoline (650 mg, 2.3 mmol) in quinoline (3 ml) was added silicon tetrachloride (0.23 ml) by a syringe at 180 °C under nitrogen atmosphere. The reaction mixture was heated at 180 °C for four hours. After cooled to room temperature, methanol (9 ml) and water (1 ml) was added to the reaction flask and the precipitates were collected by filtration. After chromatographed on alumina gel column, the compound was recrystallized from chloroform and methanol to give pure **1** as a green powder (240 mg, 36%).

MALDI-TOF-MS (*m/z*): 1150.615 ($C_{64}H_{82}SiN_8O_{10} = 1150.592 [M^+]$); UV/vis ($CHCl_3$): λ_{max} [nm] (ϵ) = 340 (66000), 359 (122000), 433 (29000), 615 (38000), 652 (37000), 682 (278000).

Dihydroxy(octakisbutoxynaphthalocyanato)silicon (2): To a suspension of 6,7-dibutoxy-1,3-diiminobenzo[f]isoindoline (1.00 g, 3.0 mmol) in quinoline (3 ml) was added silicon tetrachloride (0.23 ml) by a syringe at 180 °C under nitrogen atmosphere. The reaction mixture was heated at 180 °C for four hours. After cooled to room temperature, methanol (9 ml) and water (1 ml) was added to the reaction flask and the precipitates were collected by filtration. After chromatographed on alumina gel column, the compound was recrystallized from chloroform and methanol to give pure **2** as a green powder (130 mg, 13%).

MALDI-TOF-MS (*m/z*): 1333.564 ($C_{80}H_{89}SiN_8O_9 = 1333.652 [M^+-OH]$); UV/vis ($CHCl_3$): λ_{max} [nm] (ϵ) = 337 (151000), 358 (81000), 404 (66000), 701 (53000), 750 (52000), 790 (312000).

μ -Oxo hetero dimer of 1 and 2: **1** (22.3 mg, 19.4 μ mol) and **2** (25.5 mg, 18.9 μ mol) was dissolved in quinoline (1.5 ml), and the mixture was heated at 180 °C for three hours. Then methanol (5.0 ml) and water (1.0 ml) was added, and the precipitate was collected by filtration. The resultant solid was chromatographed on alumina gel and gel permeation column (Bio-Beads S-X1 and recycling preparative GPC-HPLC) to give SiPc-SiPc dimer **3**, SiNc-SiNc dimer **4**, and SiPc-SiNc hetero dimer **5** (20~25%).

5: HR-ESI-FT-ICR-MS (*m/z*): 2483.2306 ($C_{144}H_{170}Si_2N_{16}O_{19} = 2483.2361 [M^+]$); UV/vis ($CHCl_3$): λ_{max} [nm] = 363, 620, 681.

Axial ligand exchange reaction: **5** was reacted with triphenylsilyl chloride (20 eq) in quinoline at 180 °C for a day. After removing quinoline under vacuum, the resultant mixture was washed with hexane. The compound was purified by using gel permeation chromatography (Bio-Beads S-X1 and recycling preparative GPC-HPLC) to give **6** almost quantitatively.

6: ESI-FT-ICR-MS (*m/z*): 2724.3256 ($C_{162}H_{183}Si_3N_{16}O_{18} = 2724.3204 [M^+-OSiPh_3]$); ¹H NMR ($CDCl_3$, 600

MHz, 294 K): δ = 9.22 (s, 8H; *Nc-naphthalene*), 8.26 (s, 8H; *Pc-benzo*), 7.97 (s, 8H; *Nc-naphthalene*), 6.27 (t, 3H, J = 7.2 Hz; *axial para-phenyl*), 6.20 (t, 3H, J = 7.2 Hz; *axial para-phenyl*), 5.77 (dd, 6H, J = 7.8 Hz; *axial meta-phenyl*), 5.65 (dd, 6H, J = 7.8 Hz; *axial meta-phenyl*), 4.81 (q, 8H, J = 6.6 Hz; *Pc-methylene*), 4.61 (q, 8H, J = 7.2 Hz; *Nc-methylene*), 4.50 (m, 16H; *Nc- and Pc-methylene*), 3.99 (d, 6H, J = 6.0 Hz; *axial ortho-phenyl*), 3.85 (d, 6H, J = 6.6 Hz; *axial ortho-phenyl*), 2.43–2.39 (m, 8H; *Pc-methylene*), 2.33–2.29 (m, 8H; *Pc-methylene*), 2.22 (m, 16H; *Nc-methylene*), 2.00–1.90 (m, 16H; *Pc-methylene*), 1.88–1.81 (m, 16H; *Nc-methylene*), 1.32–1.22 ppm (t, 48H; *Nc- and Pc-methyl*); (toluene- d_8 , 600 MHz, 294 K): δ = 9.69 (s, 8H; *Nc-naphthalene*), 8.58 (s, 8H; *Pc-benzo*), 7.85 (s, 8H; *Nc-naphthalene*), 6.28 (t, 3H, J = 7.2 Hz; *axial para-phenyl*), 6.21 (t, 3H, J = 7.8 Hz; *axial para-phenyl*), 5.96 (dd, 6H, J = 7.8 Hz; *axial meta-phenyl*), 5.93 (dd, 6H, J = 6.0 Hz; *axial meta-phenyl*), 4.63 (d, 6H, J = 6.6 Hz; *axial ortho-phenyl*), 4.56 (q, 8H, J = 6.6 Hz; *Nc-methylene*), 4.36 (d, 6H, J = 6.0 Hz; *axial ortho-phenyl*), 4.30 (q, 8H, J = 6.6 Hz; *Nc-methylene*), 3.97 (q, 8H, J = 6.0 Hz; *Pc-methylene*), 3.74 (q, 8H, J = 6.6 Hz; *Pc-methylene*), 2.14–2.04 (m, 16H; *Nc-methylene*), 2.02–1.89 (m, 16H; *Pc-methylene*), 1.85 (m, 16H; *Nc-methylene*), 1.64 (m, 16H; *Pc-methylene*), 1.20–1.17 ppm (m, 48H; *Nc- and Pc-methyl*); UV/vis (CHCl_3): λ_{max} [nm] (ϵ) = 365 (45000), 618 (12000), 682 (80000), 716 (17000); (toluene): λ_{max} [nm] (ϵ) = 344 (44000), 618 (17000), 687 (43000).

ii. Space filling model of the crystal structure of 6

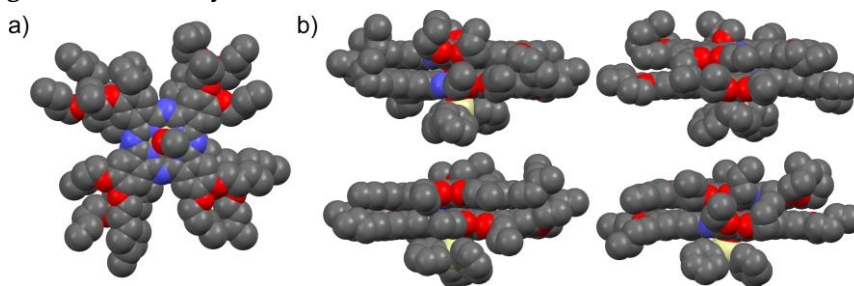


Fig. S1. Space-filling model of the crystal structure of 6, a) top view and b) side views. Hydrogen atoms are omitted for clarity.

iii. Absorption and MCD spectra of 1 and 2

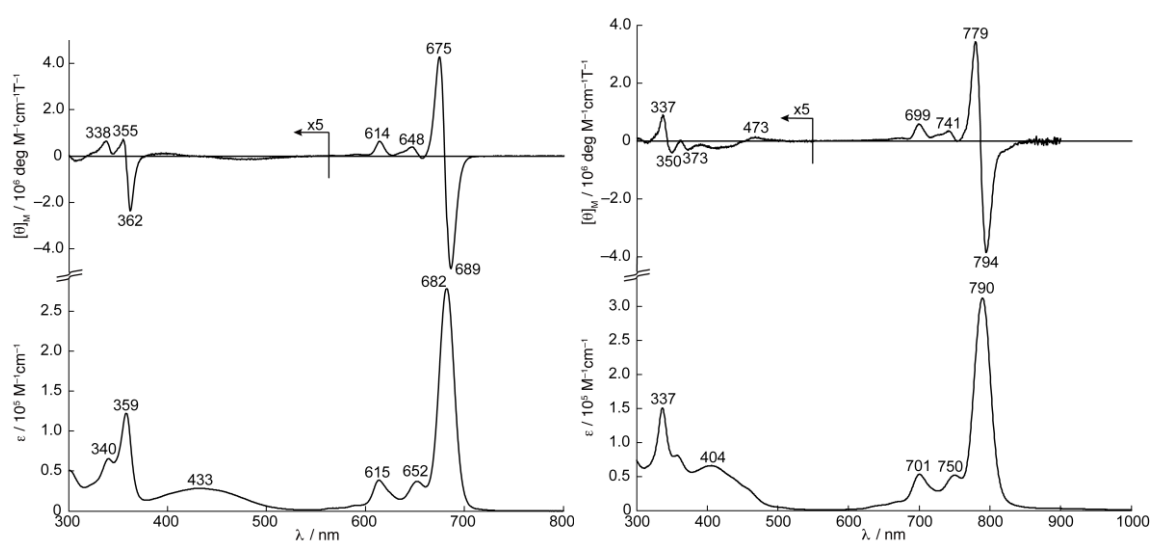


Fig. S2. Absorption (bottom) and MCD (top) spectra of 1 (left) and 2 (right) in CHCl_3 .

iv. Absorption spectra of **6** at variable concentrations

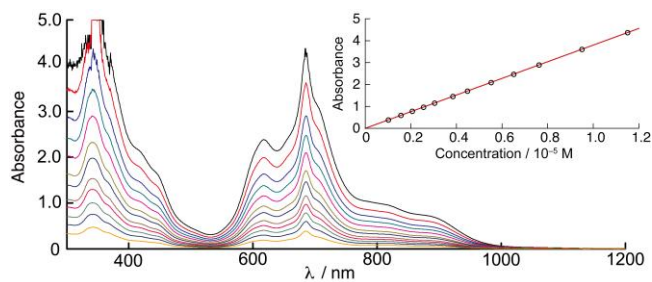


Fig. S3. Absorption spectra of **6** in toluene at variable concentrations ($1.01 \times 10^{-5} \sim 1.15 \times 10^{-4}$ M).

v. ^1H NMR spectra of **6** and variable temperature measurements

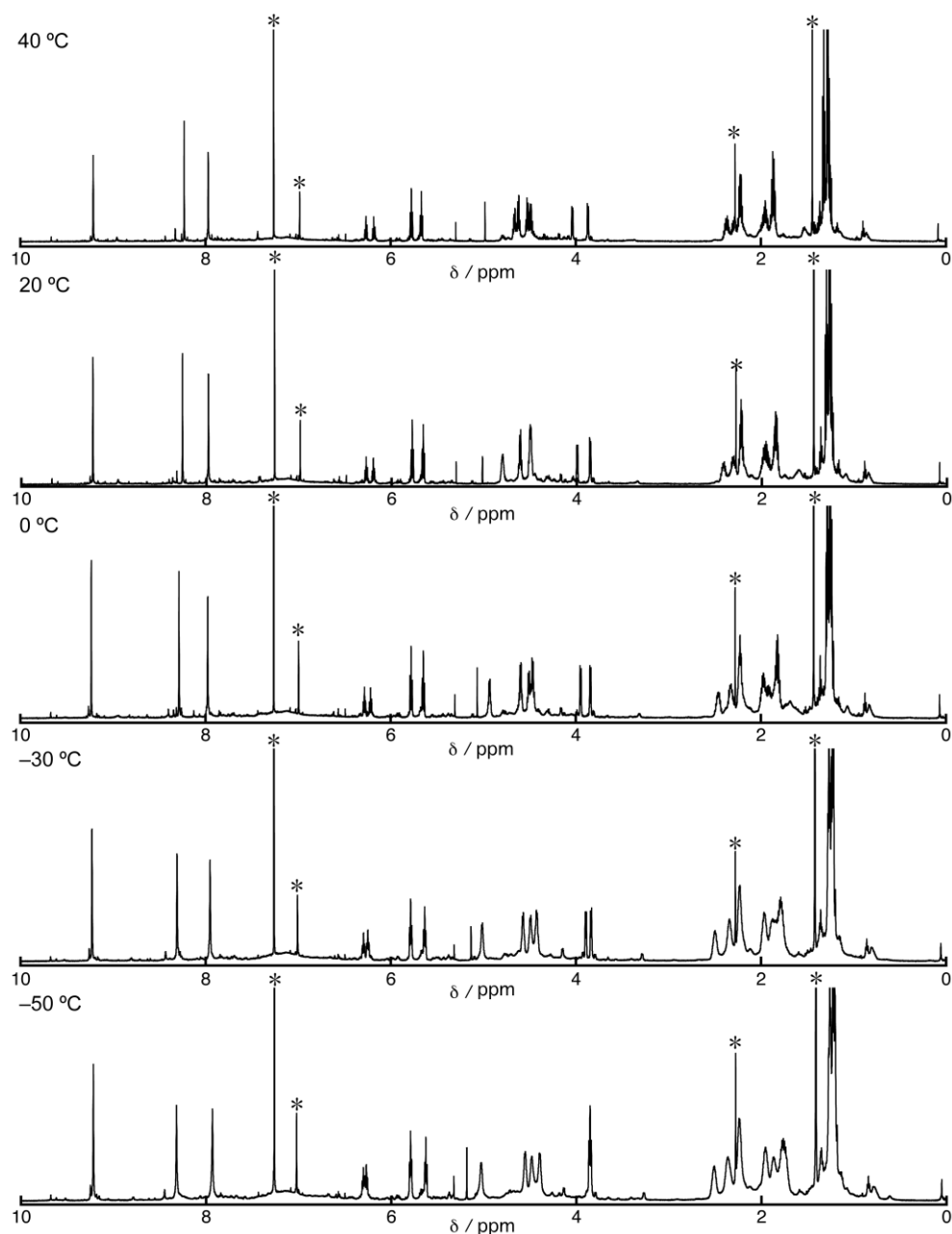


Fig. S4. ^1H NMR spectra of **6** in CDCl_3 at variable temperatures. * indicates a residual solvent peak and impurities.

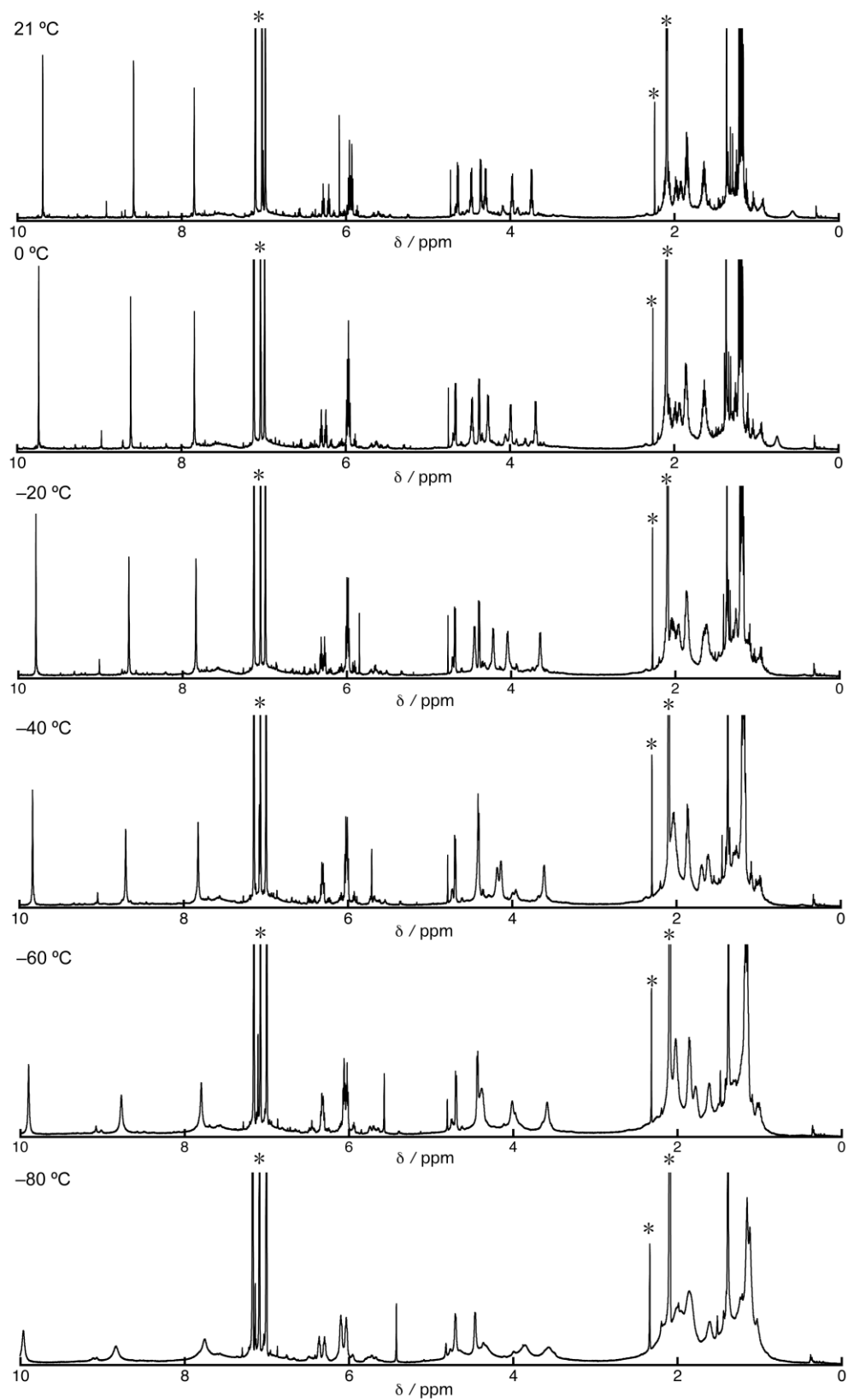


Fig. S5. ¹H NMR spectra of 6 in toluene-*d*₈ at variable temperatures. * indicates residual solvent peaks and impurities.

vi. Absorption spectra of **6** at variable temperatures

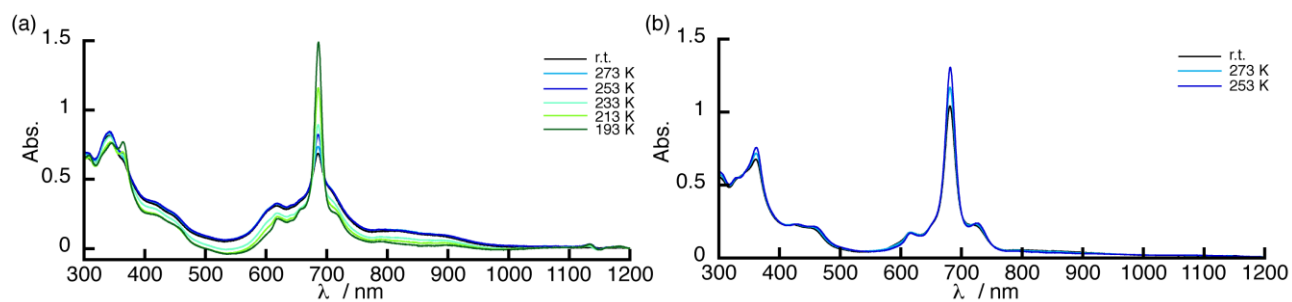


Fig. S6. Absorption spectra of **6** in (a) toluene and (b) CHCl_3 at variable temperatures.

vii. DFT and TDDFT calculations on **6**

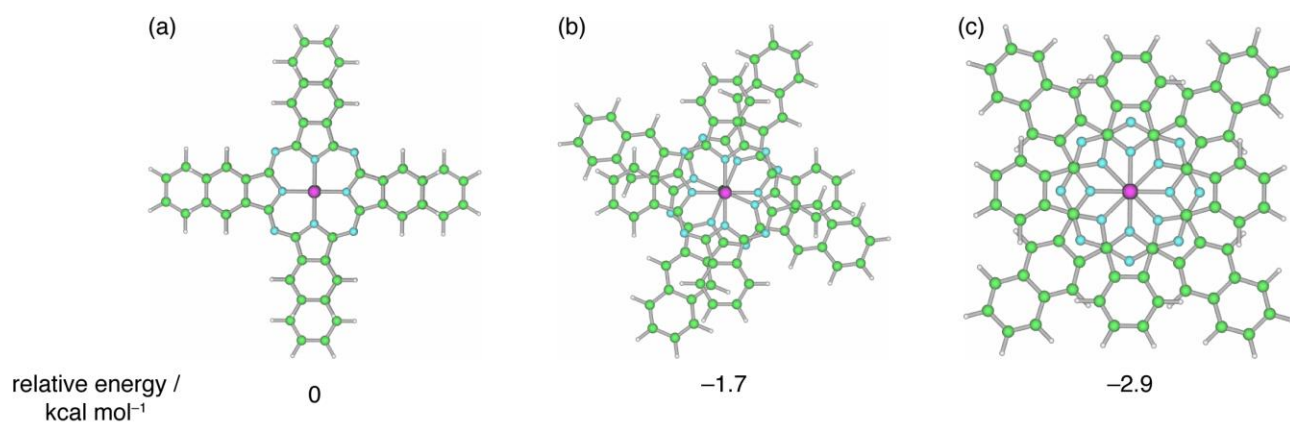


Fig. S7. Optimized structures with torsion angles of a) $\theta = 0^\circ$, b) 23° , and c) 45° .

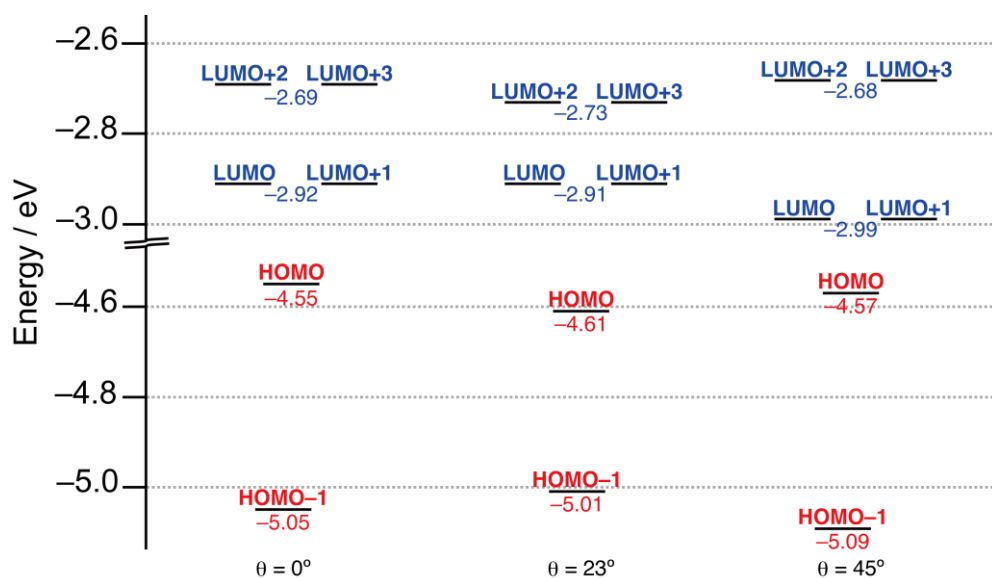


Fig. S8. Frontier molecular orbital diagrams of **6** with the torsion angles of $\theta = 0^\circ$ (left), 23° (middle), and 45° (right).

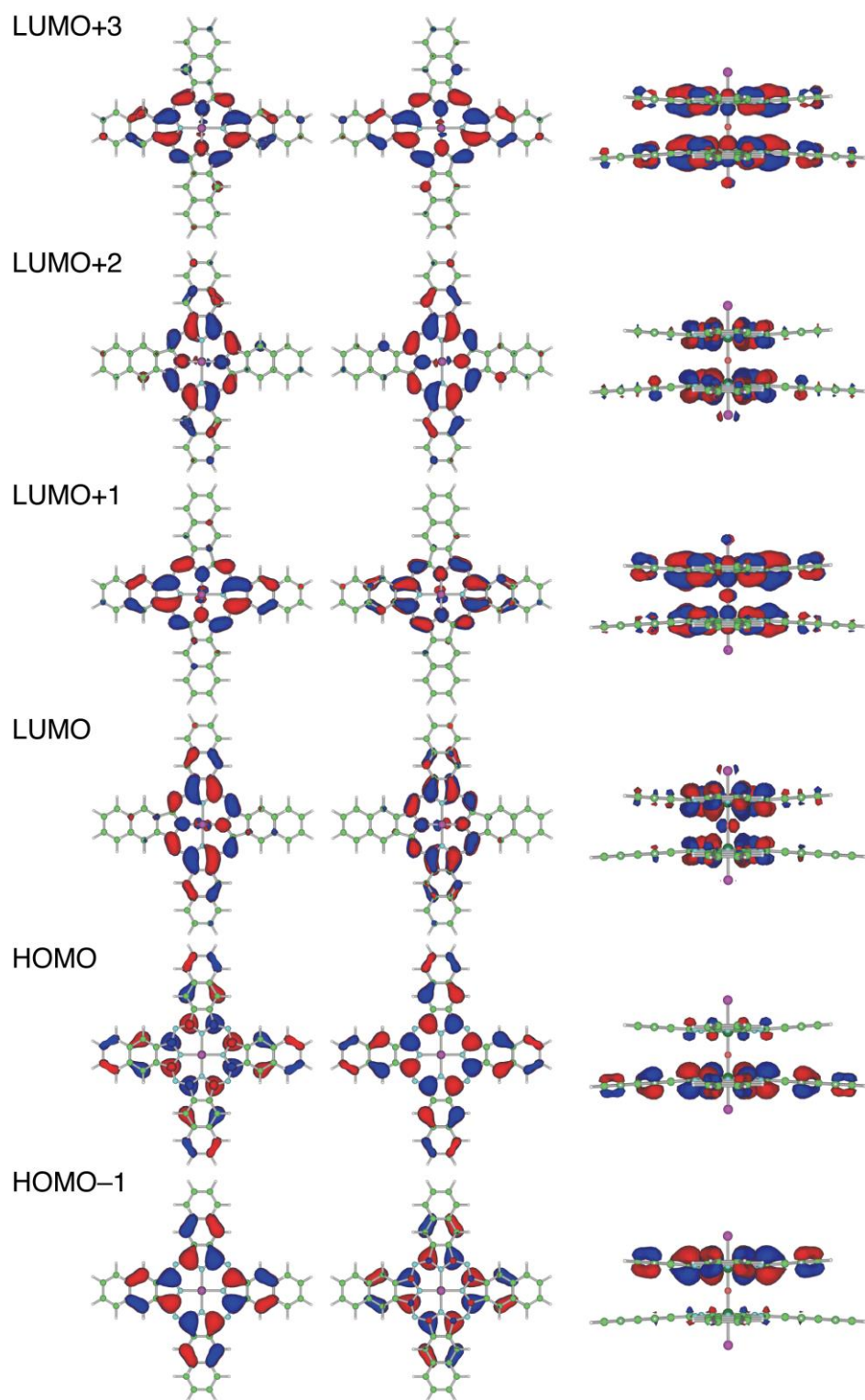


Fig. S9. Frontier molecular orbitals of **6** with the torsion angles of $\theta = 0^\circ$, top view from the Pc side (left), top view from the Nc side (middle), and side view (right).

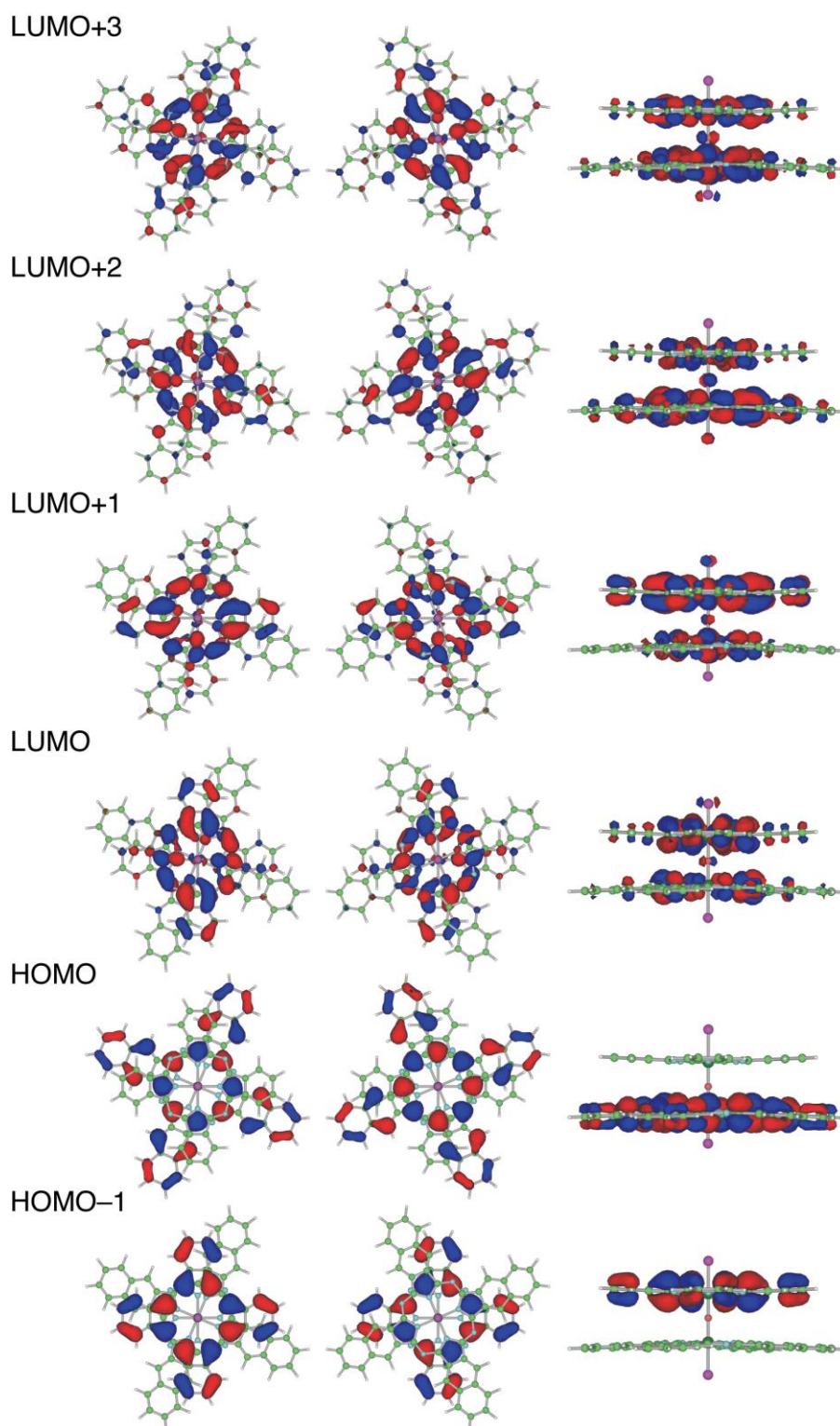


Fig. S10. Frontier molecular orbitals of **6** with the torsion angles of $\theta = 23^\circ$, top view from the Pc side (left), top view from the Nc side (middle), and side view (right).

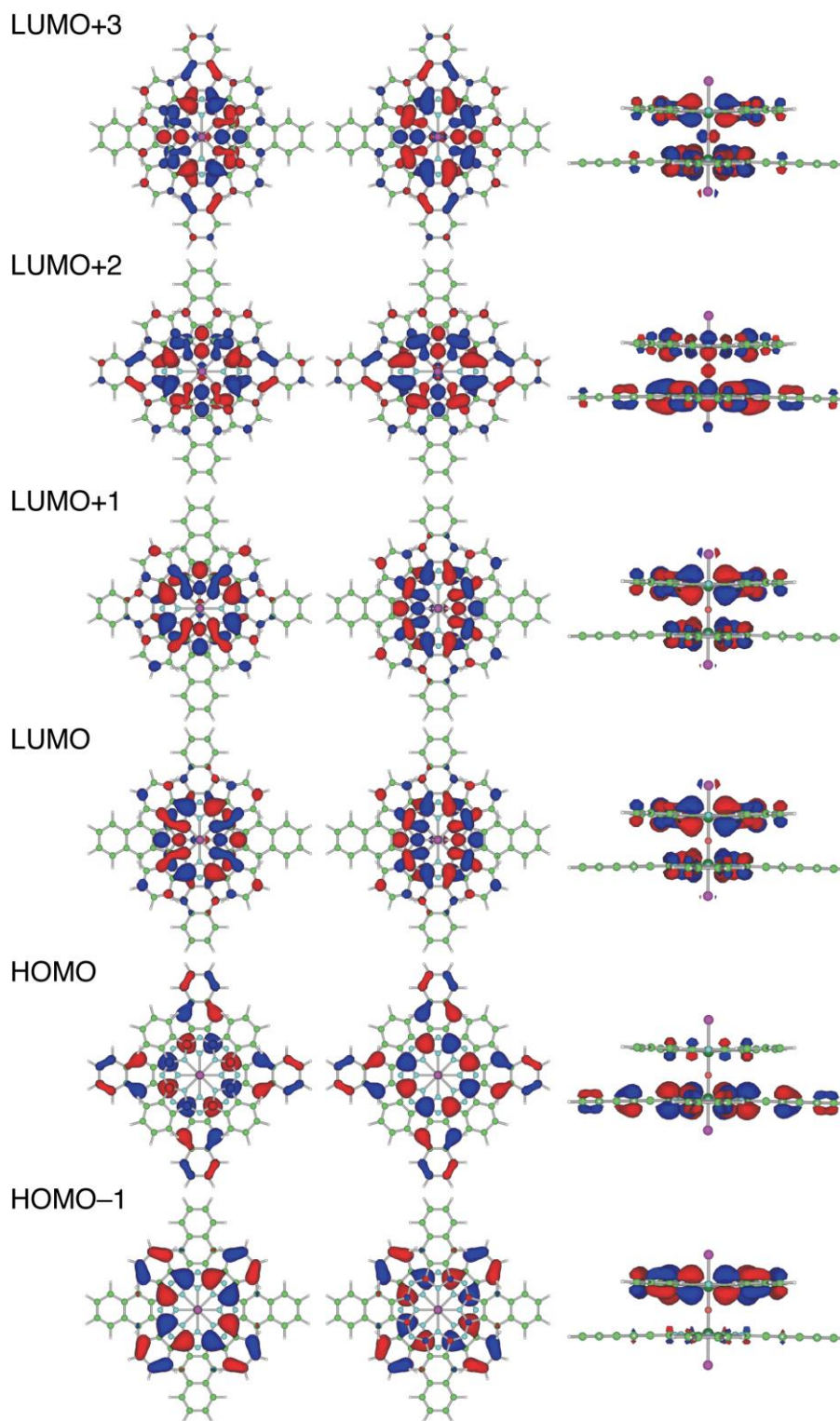


Fig. S11. Frontier molecular orbitals of 6 with the torsion angles of $\theta = 45^\circ$, top view from the Pc side (left), top view from the Nc side (middle), and side view (right).

Table S1. Selected transition energies and wave functions for **6** with the torsion angle of $\theta = 0^\circ$ calculated by the TDDFT (B3LYP/6-31G(d)) method.

	energy [nm]	$f^{[a]}$	wave function ^[b]
$\theta = 0^\circ$	1009	0.0058	+ 0.674 L \leftarrow H> - 0.205 L+2 \leftarrow H> + ...
	1009	0.0058	+ 0.675 L+1 \leftarrow H> + 0.203 L+3 \leftarrow H> + ...
	787	0.082	+ 0.572 L+2 \leftarrow H> + 0.352 L \leftarrow H-1> + 0.120 L+2 \leftarrow H-1> + 0.179 L \leftarrow H> + ...
	787	0.083	+ 0.573 L+3 \leftarrow H> - 0.352 L+2 \leftarrow H-1> + 0.121 L+3 \leftarrow H-1> - 0.178 L+1 \leftarrow H> + ...
	662	0.312	+ 0.441 L \leftarrow H-1> + 0.426 L+2 \leftarrow H-1> - 0.111 L \leftarrow H> - 0.319 L+2 \leftarrow H> + ...
	662	0.312	+ 0.440 L+1 \leftarrow H-1> - 0.427 L+3 \leftarrow H-1> - 0.110 L+1 \leftarrow H> + 0.319 L+3 \leftarrow H> + ...
	596	0.248	+ 0.537 L+2 \leftarrow H-1> - 0.402 L \leftarrow H-1> + 0.139 L+2 \leftarrow H> + ...
	596	0.248	+ 0.537 L+3 \leftarrow H-1> + 0.403 L+1 \leftarrow H-1> + 0.138 L+3 \leftarrow H> + ...

[a] Oscillator strength. [b] The wave functions based on the eigenvectors predicted by TDDFT. H and L represent the HOMO and LUMO, respectively.

Table S2. Selected transition energies and wave functions for **6** with the torsion angle of $\theta = 45^\circ$ calculated by the TDDFT (B3LYP/6-31G(d)) method.

	energy [nm]	$f^{[a]}$	wave function ^[b]
$\theta = 45^\circ$	1050	0.0090	+ 0.680 L \leftarrow H> - 0.182 L+3 \leftarrow H> + ...
	1050	0.0090	+ 0.680 L+1 \leftarrow H> + 0.182 L+2 \leftarrow H> + ...
	784	0.059	+ 0.479 L+2 \leftarrow H> - 0.197 L \leftarrow H-1> + 0.336 L+1 \leftarrow H-1> - 0.102 L+2 \leftarrow H-1> - 0.132 L+1 \leftarrow H> + 0.282 L+3 \leftarrow H> + ...
	784	0.059	+ 0.479 L+3 \leftarrow H> - 0.336 L \leftarrow H-1> - 0.197 L+1 \leftarrow H-1> - 0.102 L+3 \leftarrow H-1> + 0.132 L \leftarrow H> - 0.282 L+2 \leftarrow H> + ...
	662	0.399	+ 0.419 L+1 \leftarrow H-1> - 0.219 L \leftarrow H-1> - 0.303 L+2 \leftarrow H-1> - 0.158 L+3 \leftarrow H-1> - 0.357 L+2 \leftarrow H> - 0.170 L+3 \leftarrow H> + ...
	662	0.399	+ 0.419 L \leftarrow H-1> + 0.219 L+1 \leftarrow H-1> - 0.158 L+2 \leftarrow H-1> + 0.303 L+3 \leftarrow H-1> - 0.170 L+2 \leftarrow H> + 0.327 L+3 \leftarrow H> + ...
	589	0.183	+ 0.593 L+2 \leftarrow H-1> + 0.324 L+1 \leftarrow H-1> - 0.108 L+2 \leftarrow H> + ...
	589	0.183	+ 0.593 L+3 \leftarrow H-1> - 0.324 L \leftarrow H-1> - 0.108 L+3 \leftarrow H> + ...

[a] Oscillator strength. [b] The wave functions based on the eigenvectors predicted by TDDFT. H and L represent the HOMO and LUMO, respectively.

Table S3. Selected transition energies and wave functions for **6** with the torsion angle of $\theta = 23^\circ$ calculated by the TDDFT (B3LYP/6-31G(d)) method.

	energy [nm]	$f^{[a]}$	wave function ^[b]
$\theta = 23^\circ$	973	0.0099	+ 0.643 L \leftarrow H> - 0.278 L+2 \leftarrow H> + ...
	973	0.0099	+ 0.643 L+1 \leftarrow H> - 0.278 L+3 \leftarrow H> + ...
	743	0.169	+ 0.572 L+2 \leftarrow H> + 0.241 L \leftarrow H-1> - 0.121 L+1 \leftarrow H-1> - 0.128 L+2 \leftarrow H-1> + 0.124 L+3 \leftarrow H-1> - 0.246 L \leftarrow H> + ...
	743	0.169	+ 0.572 L+3 \leftarrow H> - 0.121 L \leftarrow H-1> - 0.241 L+1 \leftarrow H-1> - 0.124 L+2 \leftarrow H-1> - 0.128 L+3 \leftarrow H-1> + 0.246 L+1 \leftarrow H> + ...
	715	0.0646	+ 0.350 L+2 \leftarrow H-1> - 0.311 L \leftarrow H-1> - 0.345 L+1 \leftarrow H-1> - 0.304 L+3 \leftarrow H-1> + 0.147 L+2 \leftarrow H> - 0.186 L+3 \leftarrow H> + ...
	715	0.0645	+ 0.350 L+3 \leftarrow H-1> - 0.345 L \leftarrow H-1> + 0.311 L+1 \leftarrow H-1> + 0.304 L+2 \leftarrow H-1> + 0.186 L+2 \leftarrow H> + 0.147 L+3 \leftarrow H> + ...
	606	0.402	+ 0.490 L+2 \leftarrow H-1> - 0.105 L+1 \leftarrow H-9> + 0.432 L \leftarrow H-1> + 0.151 L+3 \leftarrow H> + ...
	606	0.402	+ 0.490 L+3 \leftarrow H-1> - 0.105 L \leftarrow H-9> - 0.432 L+1 \leftarrow H-1> - 0.151 L+2 \leftarrow H> + ...

[a] Oscillator strength. [b] The wave functions based on the eigenvectors predicted by TDDFT. H and L represent the HOMO and LUMO, respectively.

viii. References

- 1 M. C. Burla, R. Caliendo, M. Camalli, B. Carrozzini, G. L. Cascarano, L. D. Caro, C. Giacovazzo, G. Polidori, and R. Spagna, *J. Appl. Crystallogr.* 2005, **38**, 381.
- 2 G. M. Sheldrick, SHELXL-97, Program for the Solution and Refinement of Crystal Structures, University of Göttingen, Göttingen, Germany, 1997.
- 3 (a) A. L. Spek, *Acta Crystallogr., Sect. A* 1990, **46**, c34. (b) P. V. Sluis and A. L. Spek, *Acta Crystallogr., Sect. A* 1990, **46**, 194.
- 4 M. J. Frisch, G. W. Trucks, H. B. Schlegel, G. E. Scuseria, M. A. Robb, J. R. Cheeseman, G. Scalmani, V. Barone, B. Mennucci, G. A. Petersson, H. Nakatsuji, M. Caricato, X. Li, H. P. Hratchian, A. F. Izmaylov, J. Bloino, G. Zheng, J. L. Sonnenberg, M. Hada, M. Ehara, K. Toyota, R. Fukuda, J. Hasegawa, M. Ishida, T. Nakajima, Y. Honda, O. Kitao, H. Nakai, T. Vreven, J. A. Montgomery, Jr., J. E. Peralta, F. Ogliaro, M. Bearpark, J. J. Heyd, E. Brothers, K. N. Kudin, V. N. Staroverov, R. Kobayashi, J. Normand, K. Raghavachari, A. Rendell, J. C. Burant, S. S. Iyengar, J. Tomasi, M. Cossi, N. Rega, J. M. Millam, M. Klene, J. E. Knox, J. B. Cross, V. Bakken, C. Adamo, J. Jaramillo, R. Gomperts, R. E. Stratmann, O. Yazyev, A. J. Austin, R. Cammi, C. Pomelli, J. W. Ochterski, R. L. Martin, K. Morokuma, V. G. Zakrzewski, G. A. Voth, P. Salvador, J. J. Dannenberg, S. Dapprich, A. D. Daniels, O. Farkas, J. B. Foresman, J. V. Ortiz, J. Cioslowski, and D. J. Fox, Gaussian 09, Revision A.02, Gaussian, Inc., Wallingford CT, 2009.

ix. Acknowledgement

This work was partly supported by a Grant-in-Aid for Scientific Research on Innovative Areas (No. 20108007, "pi-Space") from MEXT. The authors thank Prof. T. Iwamoto and Dr. S. Ishida, Tohoku University for X-ray measurement, Prof. N. Teramae, Prof. S. Nishizawa, and Dr. H. Arafune, Tohoku University for low-temperature UV/vis/near-IR absorption measurement, and Prof. M. Uchiyama and Dr. A. Muranaka, RIKEN for near-IR MCD measurement.